Pramāṇa, Vol. 11, No. 4, October 1978, pp. 359–377, © printed in India

Charged particle motion in an electromagnetic field on Kerr background geometry

A R PRASANNA and C V VISHVESHWARA*
Physical Research Laboratory, Ahmedabad 380 009
*Raman Research Institute, Bangalore 560 006

MS received 5 April 1978

Abstract. In this paper we study the trajectories of charged particles in an electromagnetic field superimposed on the Kerr background. The electromagnetic fields considered are of two types: (i) a dipole magnetic field with an associated quadrupole electric field, (ii) a uniform magnetic field. The contribution of the background geometry to the electromagnetic field is taken through the solutions of Petterson and Wald respectively. The effective potential is studied in detail for the r-motion of the particles in the equatorial plane and the orbits are obtained. The most interesting aspect of the study is the illustration of the effect of inertial frame dragging due to the rotation of the central star. This appears through the existence of nongyrating bound orbits at and inside the ergo surface. The presence of the magnetic field seems to increase the range of stable orbits, as was found in a previous study involving the Schwarzschild background.

Keywords. Charged particle orbits; Kerr geometry; pulsars, general relativity.

1. Introduction

There has been considerable interest in the investigation of electromagnetic fields surrounding compact objects like neutron stars and black holes. Such studies shed light on the interplay of electromagnetism and the curvature of spacetime due to strong gravitational fields. Furthermore, they provide the basis for astrophysical applications if relevant situations occur. In this context, the investigation of the trajectories of charged particles can reveal the influence of the geometry on the electromagnetic fields, just as the study of geodesics yields important information regarding the structure of spacetime (Barden 1972, Bicak and Stuchilk 1976). At the same time, it would constitute the orbit theory of the test charges which is the first step towards the examination of possible plasma processes near collapsed objects.

The charged particle trajectories in a dipole magnetic field superposed on the Schwarzschild background geometry have already been considered in a recent paper (Prasanna and Varma 1977). There it was found that the presence of magnetic field increases the range of stable orbits. It is known that almost all of the celestial bodies do have a non-zero angular momentum and thus the Schwarzschild geometry does not tell the whole story. Thus it is necessary to extend the studies of the charged particle orbits to the case of Kerr background with an electromagnetic field. The electromagnetic fields that we consider are of two types:

(i) a dipole magnetic field with an associated (induced) quadrupole electric field due to the rotation of the central star; (higher multipoles) $\gtrsim O(a^2)$ are assumed to be negligible.

(ii) a uniform magnetic field surrounding the central star, which is constant at infinity.

2. Field structure

The space-time metric for the external field of a rotating star of mass M and angular velocity a is given by the Kerr solution which in Boyer-Lindquist coordinates may be written as,

$$ds^2 = -\left(1 - \frac{2mr}{\Sigma}\right) c^2 dt^2 - \frac{4mra}{\Sigma} \sin^2\theta \, dt \, d\varphi + (\Sigma/\triangle)\, dr^2 + \Sigma d\theta^2 + (B/\Sigma) \sin^2\theta \, d\varphi^2, \tag{1}$$

where

$$\Sigma = (r^2 + a^2 \cos^2\theta), \quad \triangle = (r^2 + a^2 - 2mr), \; m = \frac{MG}{c^2}$$

$$B = (r^2 + a^2)^2 - \triangle a^2 \sin^2 \theta.$$

Case 1.

Several authors have obtained the solution for a stationary axisymmetric electromagnetic field around a rotating black hole by using Teukolsky's perturbation equations in the Newman-Penrose formalism (Chitre and Vishveshwara 1975; Petterson 1975; King *et al* 1975). We shall use the expression for the vector potential as given by Petterson restricting ourselves to the case of a dipole magnetic field with no electrostatic charge ($Q = 0$) which is given by

$$A_i = (A_t, 0, 0, A_\varphi) \tag{2}$$

$$A_t = \left(\frac{a\beta_1{}^i}{\Sigma}\right)\left\{[r(r-m) + (a^2 - mr)\cos^2\theta] \frac{1}{2\gamma} \ln\left(\frac{r-m+\gamma}{r-m-\gamma}\right) - (r - m\cos^2\theta)\right\} - \left(\frac{\beta_1{}^r \cos\theta}{\Sigma}\right)\left\{(a^2 \sin^2\theta - r^2 + mr) + [(r^3 - 2mr^2 + ma^2) + (r-m)a^2 \cos^2\theta] \frac{1}{2\gamma} \ln\left(\frac{r-m+\gamma}{r-m-\gamma}\right)\right\}. \tag{3}$$

$$A_\varphi = \left(\frac{\beta_1{}^i \sin^2\theta}{2\Sigma}\right)\left\{ r(r^2 + mr + 2a^2) + (r-m)\, a^2 \cos^2\theta - [r(r^3 - 2ma^2 + a^2 r) + \triangle a^2 \cos^2\theta] \frac{1}{2\gamma} \ln\left(\frac{r-m+\gamma}{r-m-\gamma}\right)\right\} + \left(\frac{a\beta_1{}^r \sin^2\theta \cos\theta}{\Sigma}\right)\left\{(a^2 + mr) + \frac{m(a^2 - r^2)}{2\gamma} \ln\left(\frac{r-m+\gamma}{r-m-\gamma}\right)\right\}, \tag{4}$$

with $\gamma = (m^2 - a^2)^{1/2}$, $\beta_1{}^r$, and $\beta_1{}^i$ being constants.

From previous work (Prasanna and Varma 1977) concerning dipole magnetic field on the Schwarzschild background, we know that in the absence of rotation ($a = 0$) there is no electric field and $A_t = 0$. This requires immediately the constant $\beta_1{}^r = 0$. In order to determine $\beta_1{}^i$, we consider the boundary condition, that the Kerr geometry is asymptotically flat and thus as $r \to \infty$ the magnetic field and the electric field should have the structure of dipole and quadrupole fields on flat spacetime respectively. Accordingly we get,

$$\beta_1{}^i = \mp (3\mu/2\gamma^2) \tag{5}$$

depending on whether the dipole moment μ is parallel or antiparallel to the rotation axis. However in our study we shall consider only the case with $\beta_1{}^i = -3\mu/2\gamma^2$. Hence we get the components of the vector potential to be

$$A_t = \left(-\frac{3a\mu}{2\gamma^2 \Sigma} \right) \left\{ [r(r-m) + (a^2 - mr) \cos^2 \theta] \cdot \frac{1}{2\gamma} \ln \left(\frac{r-m+\gamma}{r-m-\gamma} \right) - (r - m \cos^2 \theta) \right\}. \tag{6}$$

$$A_\varphi = \left(-\frac{3\mu \sin^2 \theta}{4\gamma^2 \Sigma} \right) \left\{ (r-m)a^2 \cos^2 \theta + r(r^2 + mr + 2a^2) - [r(r^3 - 2ma^2 + a^2 r) + \triangle a^2 \cos^2 \theta] \frac{1}{2\gamma} \ln \left(\frac{r-m+\gamma}{r-m-\gamma} \right) \right\}. \tag{7}$$

Case 2. *Uniform magnetic field*

Wald (1974) has studied the case of a black hole in a uniform magnetic field, by using the fact that a Killing vector in an empty space time serves as a vector potential for a Maxwell test field. He has derived the solution for the electromagnetic field when a stationary, axisymmetric black hole is placed in an originally uniform magnetic field aligned along the symmetry axis of the black hole. We shall now use this solution for studying the charged particle orbits. We shall again assume that there is no electrostatic charge ($Q = 0$). This would give us the vector potential to be

$$A_i = (B_0/2) \left(\psi_i + \frac{2J}{M} \eta_i \right), \tag{8}$$

where ψ_i is the space-like and η_i the time-like Killing vectors. As the background geometry is that of Kerr we get the explicit solution as

$$A_t = -aB_0 \left[1 - \frac{mr}{\Sigma} (2 - \sin^2 \theta) \right]$$

$$A_\varphi = \frac{B_0 \sin^2 \theta}{2\Sigma} \{ (r^2 + a^2)^2 - \triangle a^2 \sin^2 \theta - 4ma^2 r \} \tag{9}$$

B_0 being the magnetic field strength.

3. Equations of motion

As both the gravitational and the electromagnetic fields are axisymmetric and stationary, there exist two Killing vectors such that for the motion of a charged

particle of charge e and rest mass M_0, there are two constants of motion, the canonical angular momentum l and energy E as given by

$$(U_\varphi + eA_\varphi) = l, \tag{10}$$

$$(U_t + eA_t) = -E, \tag{11}$$

wherein all quantities are normalised with respect to the particle rest mass M_0. U_t and U_φ are connected with the components of particles proper velocity U^i as follows:

$$U^t = -[BU_t + 2amrU_\varphi]/\Sigma\triangle$$

$$U^\varphi = [(\Sigma - 2mr)U_\varphi/\sin^2\theta - 2amrU_t]/\Sigma\triangle. \tag{12}$$

Using these in the general equations of motion of a charged particle in the presence of an external force field

$$U^b \nabla_b U_a = eF_{ab}U^b, \tag{13}$$

with $F_{ab} = (A_{b,a} - A_{a,b})$.
We get the explicit equations:

$$\begin{aligned}
&\frac{d^2r}{ds^2} - \frac{[m(r^2 - a^2\cos^2\theta) - ra^2\sin^2\theta]}{\Sigma\triangle}\left(\frac{dr}{ds}\right)^2 \\
&- \frac{2a^2\sin\theta\cos\theta}{\Sigma}\frac{dr}{ds}\frac{d\theta}{ds} - \frac{r\triangle}{\Sigma}\left(\frac{d\theta}{ds}\right)^2 + \frac{m\triangle}{\Sigma^3}(r^2 - a^2\cos^2\theta)\left(\frac{dt}{ds}\right)^2 \\
&- \frac{\triangle\sin^2\theta}{\Sigma^3}\{r^5 + 2r^3a^2\cos^2\theta - mr^2a^2\sin^2\theta + (m-r)a^4\sin^2\theta\cos^2\theta \\
&+ ra^4\cos^2\theta\}\left(\frac{d\varphi}{ds}\right)^2 \\
&- \frac{2\triangle am\sin^2\theta\,(r^2 - a^2\cos^2\theta)}{\Sigma^3}\frac{d\varphi}{ds}\frac{dt}{ds} \\
&\quad = \frac{e}{M_0}\frac{\triangle}{\Sigma}\left\{A_{\varphi,r}\frac{d\varphi}{ds} + A_{t,r}\frac{dt}{ds}\right\},
\end{aligned} \tag{14}$$

$$\begin{aligned}
&\frac{d^2\theta}{ds^2} + \frac{a^2\sin\theta\cos\theta}{\Sigma\triangle}\left(\frac{dr}{ds}\right)^2 + \frac{2r}{\Sigma}\frac{dr}{ds}\frac{d\theta}{ds} - \frac{a^2\sin\theta\cos\theta}{\Sigma}\left(\frac{d\theta}{ds}\right)^2 \\
&+ \frac{4mra\,(r^2+a^2)}{\Sigma^3}\sin\theta\cos\theta\frac{d\varphi}{ds}\frac{dt}{ds} - \frac{2mra^2}{\Sigma^3}\sin\theta\cos\theta\left(\frac{dt}{ds}\right)^2 \\
&- \frac{\sin\theta\cos\theta}{\Sigma^3}[(r^2+a^2)^3 - (r^2+a^2+\Sigma)\triangle a^2\sin^2\theta]\left(\frac{d\varphi}{ds}\right)^2 \\
&\quad = \frac{e}{M_0}\frac{1}{\Sigma}\left\{A_{\varphi,\theta}\frac{d\varphi}{ds} + A_{t,\theta}\frac{dt}{ds}\right\},
\end{aligned} \tag{15}$$

$$\frac{d\varphi}{ds} = \frac{1}{\triangle\sin^2\theta}\left\{\left(1 - \frac{2mr}{\Sigma}\right)(l - A_\varphi) + 2mra\sin^2\theta\,(E + A_t)/\Sigma\right\} \tag{16}$$

$$\frac{dt}{ds} = \frac{1}{\triangle}\left\{-\frac{2mra}{\Sigma}(l - A_\varphi) + [(r^2+a^2)^2 - \triangle a^2\sin^2\theta]\sin^2\theta\,(E + A_t)/\Sigma\right\}. \tag{17}$$

Introducing dimensionless quantities

$$\rho = r/m, \quad \sigma = s/m, \quad a = a/m,$$
$$L = l/m, \quad \tau = ct/m, \quad \bar{A}_\varphi = A_\varphi/m, \tag{18}$$

and rewriting the above equations we get:

$$\frac{d^2\rho}{d\sigma^2} - \frac{[\rho^2 - a^2\cos^2\theta - \rho a^2 \sin^2\theta]}{\Sigma\Delta}\left(\frac{d\rho}{d\sigma}\right)^2 - \frac{\rho\Delta}{\Sigma}\left(\frac{d\theta}{d\sigma}\right)^2$$
$$- \frac{2a^2\sin\theta\cos\theta}{\Sigma}\left(\frac{d\rho}{d\sigma}\right)\left(\frac{d\theta}{d\sigma}\right) - \frac{\Delta}{\Sigma^3}(\rho^2 - a^2\cos^2\theta)\left(\frac{d\tau}{d\sigma}\right)^2$$
$$- 2\frac{\Delta a \sin^2\theta}{\Sigma^3}(\rho^2 - a^2\cos^2\theta)\left(\frac{d\varphi}{d\sigma}\right)\left(\frac{d\tau}{d\sigma}\right) \tag{19}$$
$$- \frac{\Delta\sin^2\theta}{\Sigma^3}\{\rho^5 + 2\rho^3 a^2\cos^2\theta - \rho^2 a^2\sin^2\theta + (1-\rho)a^4\sin^2\theta\cos^2\theta$$
$$+ \rho a^4\cos^2\theta\}\left(\frac{d\varphi}{d\sigma}\right)^2$$
$$= \left(\frac{\Delta}{\Sigma}\right)\left\{\frac{d\bar{A}_\varphi}{d\rho}\frac{d\varphi}{d\sigma} + \frac{dA_\tau}{d\rho}\frac{d\tau}{d\sigma}\right\} \cdot \frac{d^2\theta}{d\sigma^2}$$
$$+ \frac{a^2\sin\theta\cos\theta}{\Sigma\Delta}\left(\frac{d\rho}{d\sigma}\right)^2 + \frac{2\rho}{\Sigma}\left(\frac{d\rho}{d\sigma}\right)\left(\frac{d\theta}{d\sigma}\right)$$
$$- \frac{a^2\sin\theta\cos\theta}{\Sigma}\left(\frac{d\theta}{d\sigma}\right)^2 - \frac{2\rho a^2\sin\theta\cos\theta}{\Sigma^3}\left(\frac{d\tau}{d\sigma}\right)^2$$
$$+ \frac{4\rho a(\rho^2+a^2)}{\Sigma^3}\sin\theta\cos\theta\left(\frac{d\varphi}{d\sigma}\right)\left(\frac{d\tau}{d\sigma}\right) - \frac{\sin\theta\cos\theta}{\Sigma^3}[(\rho^2+a^2)^3$$
$$- (\rho^2+a^2+\Sigma)\,\Delta a^2\sin^2\theta]\left(\frac{d\varphi}{d\sigma}\right)^2$$
$$= \frac{1}{\Sigma}\left(\frac{d\bar{A}^\varphi}{d\theta}\frac{d\varphi}{d\sigma} + \frac{dA_\tau}{d\theta}\frac{d\tau}{d\sigma}\right) \tag{20}$$

$$\frac{d\varphi}{d\sigma} = \left(\frac{1}{\Delta\Sigma}\right)\{(\Sigma - 2\rho)\,(L - \bar{A}_\varphi)/\sin^2\theta + 2\rho a\,(E + A_\tau)\}. \tag{21}$$

$$\frac{d\tau}{d\sigma} = \left(\frac{1}{\Delta\Sigma}\right)\{[(\rho^2+a^2)^2 - \Delta a^2\sin^2\theta]\,(E + A_\tau) - 2\rho a\,(L - \bar{A}_\varphi)\}. \tag{22}$$

wherein A_τ and $\bar{A}_\varphi$ are taken appropriate to the case under consideration.

4. Motion in the equatorial plane

The motion in the equatorial plane may be characterised by the equations of motion obtained earlier for the particular θ value, $\theta = \pi/2$, $(d\theta/d\sigma) = 0$. The motion is completely determined dy L, E and the space-time metric (1). Using (10) and (11) in (8) we get:

$$(U^\rho)^2 \equiv (d\rho/d\sigma)^2 = 1/\rho^3 \{[\rho(\rho^2+a^2) + 2a^2](E+A_\tau)^2 - 4a(E+A_\tau)(L-\bar{A}_\varphi) - (\rho-2)(L-\bar{A}_\varphi)^2 - \rho\triangle\}. \quad (23)$$

Following Bardeen (1972) we define the effective potential for ρ-motion by solving for the turning points of the orbits given by $U^\rho = 0$. Thus we get

$$V_{\text{eff}} = E_{\min} = -A_\tau + K/R, \quad (24)$$

with

$$K = [2a(L-\bar{A}_\varphi) + \triangle^{1/2}\{\rho^2(L-\bar{A}_\varphi)^2 + \rho R\}^{1/2}]$$
$$R = (\rho^3+a^2\rho+2a^2), \quad \triangle = (\rho^2-2\rho+a^2) \quad (25)$$

Using the expressions for A_τ and $\bar{A}_\varphi$ for the two different cases we can write $V_{\text{eff}} = F(\rho)$ as a function of ρ and study the effective potential curves.

Case 1

As given in section 2, we have for this case the vector potential A_i from (6) and (7) expressed in terms of ρ, σ, ... by

$$A_\tau = \left(\frac{-3\lambda a}{4(1-a^2)^{3/2}}\right)\left\{\left(1-\frac{1}{\rho}\right)\ln\left(\frac{\rho-1+\sqrt{1-a^2}}{\rho-1-\sqrt{1-a^2}}\right) - (2\sqrt{1-a^2})/\rho\right\} \quad (26)$$

$$\bar{A}_\varphi = \left(\frac{-3\lambda}{8(1-a^2)^{3/2}}\right)\left\{2(\sqrt{1-a^2})(1+\rho+(2a^2/\rho)) - \left(\rho^2+a^2-\frac{2a^2}{\rho}\right)\ln\left(\frac{\rho-1+\sqrt{1-a^2}}{\rho-1-\sqrt{1-a^2}}\right)\right\}, \quad (27)$$

where $\lambda = e\mu/m^2$.

Figures 1 to 7 show the plots of F as a function of ρ for different values of a, λ and L. From the expressions for A_τ and $\bar{A}_\varphi$, it is apparent that both of them have logarithmic singularities at $\rho = 1+\sqrt{1-a^2}$, the event horizon. This reflects in the

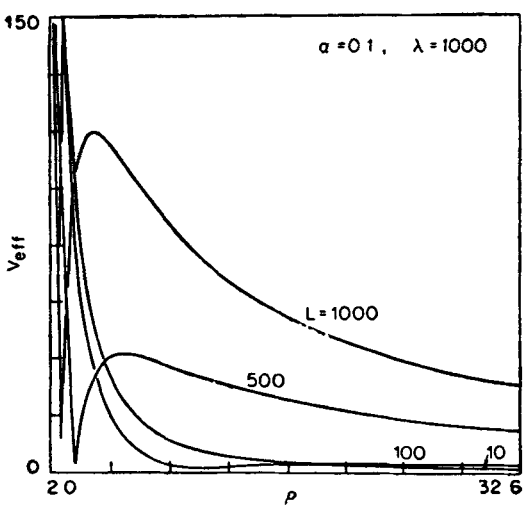

Figure 1.

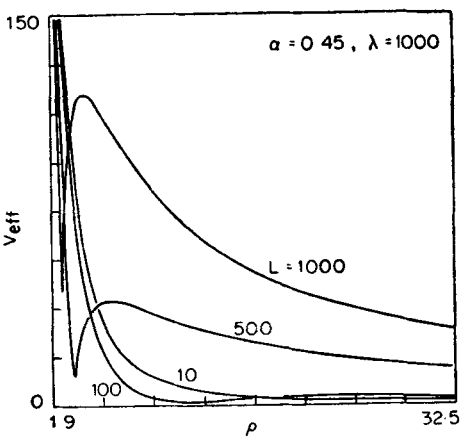

Figure 2.

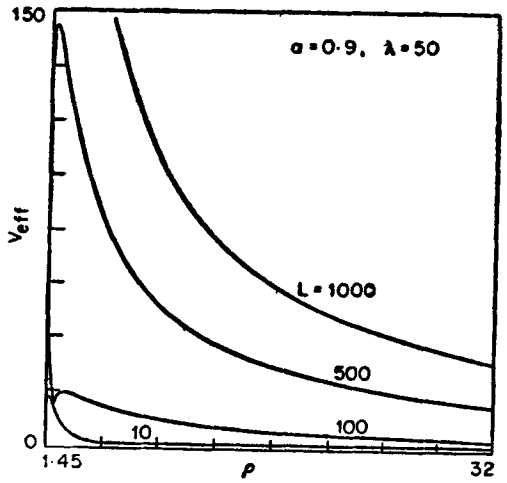

Figure 3.

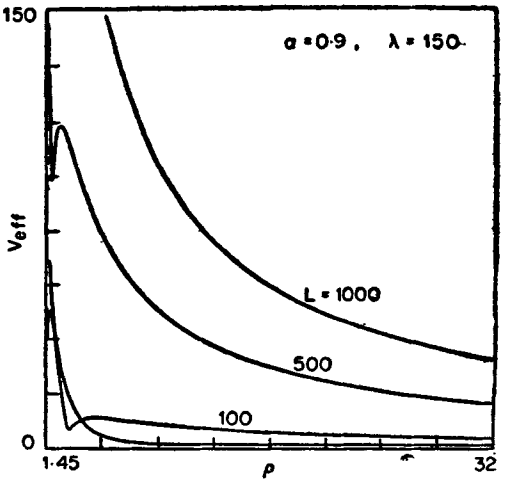

Figure 4.

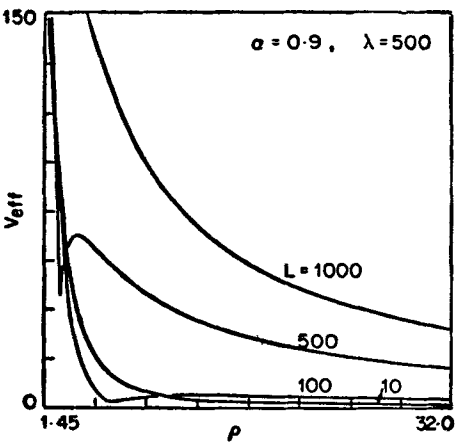

Figure 5.

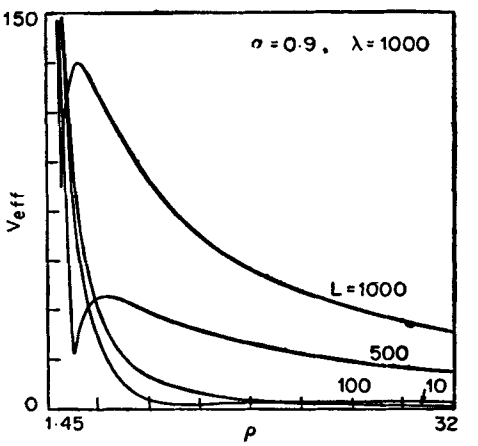

Figure 6.

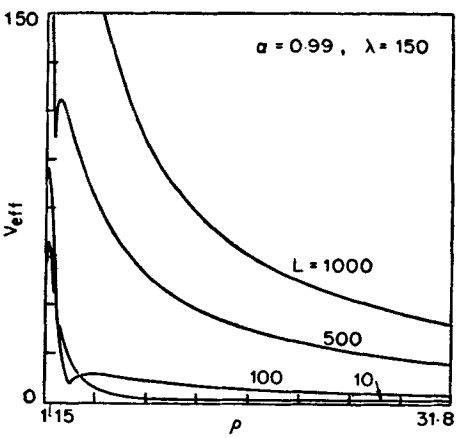

Figure 7.

Figures 1-7. Plots of effective potential as a function of ρ for different values of α, λ and L for the case of dipole magnetic field.

effective potential having a maximum very near the event horizon. The V_{eff}, then decreases sharply to a minimum and then rises to a second maximum which is indeed the centrifugal barrier (increases with increasing L) after which it smoothens out towards a flat minimum at large distances.

Table 1. $\alpha = 0{\cdot}1$ $\bar{\rho} = 1{\cdot}99508$

λ	L	M_1	ρ_{M_1}	m	ρ_m	M_2	ρ_{M_2}
	10	12·8192	2·08423	0·842611	6·28404	1·01198	16·8720
	100	8·59854	2·01456	1·84804	2·18804	14·4595	3·76862
50	500		$<\bar{\rho}$	11·6013	1·99559	93·1164	3·04509
	1000		$<\bar{\rho}$		$<\bar{\rho}$	193·034	2·96226
	10	40·0452	2·09604	0·936031	14·9605	—	>30
	100	33·7370	2·05342	1·24632	3·08303	9·21090	5·71800
150	500	23·0221	2·00229	9·73257	2·05606	81·4313	3·39620
	1000	26·5905	1·99573	22·2353	2·00061	179·838	3·13020
	10	80·9224	2·09926	0·965100	26·7526	—	>30
	100	73·9496	2·07384	1·02406	4·54706	5·98416	8·70652
300	500	54·3433	2·02037	7·35614	2·26613	68·3250	3·95643
	1000	46·0439	2·00229	19·2934	2·05606	162·859	3·39615
	10	135·433	2·10058	—	>30	—	>30
	100	128·176	2·08417	0·96063	6·53117	4·12090	12·7139
500	500	103·591	2·03879	5·32077	2·61399	56·1497	4·72990
	1000	85·9785	2·01455	15·8164	2·18795	144·429	3·76680
	10	271·714	2·10159	—	>30	—	>30
	100	264·238	2·09291	0·948504	11·5165	2·42389	22·7725
1000	500	235·184	2·06276	3·01195	3·56470	38·7794	6·70403
	1000	207·182	2·03879	10·1563	2·61391	112·292	4·72980

Table 2. $\alpha = 0{\cdot}45$ $\bar{\rho} = 1{\cdot}893128$

λ	L	M_1	ρ_{M_1}	m	ρ_m	M_2	ρ_{M_2}
	10	12·8915	2·00838	0·890279	6·47308	1·01526	15·8422
	100	16·0621	1·91819	7·32076	2·13430	15·9340	3·34908
50	500	55·4341	1·89328	54·4258	1·89491	108·095	2·58653
	1000	226·193	2·50157		$<\bar{\rho}$		$<\bar{\rho}$
	10	38·8490	2·02607	0·944468	15·4044	—	30
	100	39·2957	1·96595	3·50699	3·07200	9·67194	5·36061
150	500	62·9607	1·90344	43·9813	1·98042	91·6956	2·95633
	1000	111·207	1·89454	103·542	1·90469	206·972	2·67530
	10	77·8445	2·03104	0·967891	27·4247	—	>30
	100	77·3244	1·99352	1·97846	4·55540	6·14818	8·38249
300	500	90·4896	1·92509	31·8993	2·21900	74·6853	3·54696
	1000	125·921	1·96344	87·7699	1·98036	183·388	2·95630
	10	129·850	2·03310	—	>30	—	>30
	100	128·898	2·00831	1·40363	6·55359	4·18971	12·4048
500	500	135·665	1·94740	22·0918	2·58623	59·9668	4·35004
	1000	160·615	1·91818	70·4128	2·13311	159·191	3·34792
	10	259·873	2·03466	—	>30	—	>30
	100	258·577	2·02131	1·40363	6·55359	2·44318	22·4631
1000	500	259·138	1·97830	22·0918	2·58623	59·9668	6·36417
	1000	271·330	1·94740	43·6967	2·58581	119·926	4·34997

Table 3. $a = 0{\cdot}9$ $\bar{\rho} = 1{\cdot}435989$

λ	L	M_1	ρ_{M_1}	m	ρ_m	M_2	ρ_{M_2}
	10	17·1867	1·59150	0·945115	6·77408	1·02038	14·5054
	100	36·2314	1·49113	14·3917	1·97054	18·4438	2·75584
50	500	145·172	1·44383	128·928	1·49905	145·060	1·79727
	1000	293·991	1·43758	285·360	1·44918	316·975	1·66985
	10	48·3268	1·61315	0·954271	16·0461	—	>30
	100	64·4536	1·54413	6·25395	3·03131	10·3195	4·89495
150	500	158·361	1·47070	91·9033	1·73788	111·455	2·29320
	1000	293·124	1·45100	234·375	1·55799	268·644	1·92509
	10	95·1208	1·61951	0·971178	28·35334	—	>30
	100	110·039	1·57438	3·15455	4·55925	6·36627	7·96648
300	500	193·913	1·49940	62·9132	2·07667	85·0729	2·97920
	1000	316·722	1·47070	183·554	1·73757	222·907	2·29320
	10	157·530	1·62218	—	>30	—	>30
	100	171·859	1·59147	1·95629	6·58202	4·27962	12·0086
500	500	249·071	1·52421	42·5962	2·50276	65·6272	3·84514
	1000	362·312	1·49112	140·839	1·96584	184·298	2·75563
	10	313·567	1·62423	—	>30	—	>30
	100	327·401	1·60720	1·25833	11·6342	2·46823	22·0653
1000	500	397·422	1·55751	21·1167	3·52571	42·4210	5·92552
	1000	498·141	1·52421	84·7074	2·50169	131·247	3·84513

Table 4. $a = 0{\cdot}99$ $\bar{\rho} = 1{\cdot}141167$

λ	L	M_1	ρ_{M_1}	m	ρ_m	M_2	ρ_{M_2}
	10	22·7096	1·28234	0·955089	6·84573	1·02155	14·2328
	100	53·6887	1·21282	15·7641	1·92745	19·0441	2·63176
50	500	207·965	1·16871	149·605	1·36570	158·687	1·58328
	1000	410·321	1·15670	345·581	1·26304	358·907	1·40367
	10	61·9672	1·29757	0·956090	16·1857	—	>30
	100	90·8909	1·25012	6·76826	3·02038	10·4554	4·80183
150	500	234·881	1·19658	101·916	1·67119	116·721	2·14703
	1000	426·653	1·17774	266·489	1·45206	288·604	1·73914
	10	120·921	1·30215	0·971808	28·5487	—	>30
	100	148·937	1·27062	3·37956	4·55934	6·41064	7·88363
300	500	286·134	1·21896	68·8432	2·03911	87·4797	2·86203
	1000	469·762	1·19658	203·568	1·67075	233·439	2·14704
	10	199·542	1·30409	—	>30	—	>30
	100	227·095	1·28234	2·06368	6·58777	4·29775	11·9296
500	500	359·661	1·23651	46·4349	2·48079	66·8543	3·74335
	1000	536·886	1·21282	154·526	1·92139	190·298	2·63182
	10	396·103	1·30559	—	>30	—	>30
	100	423·254	1·29334	1·29227	11·6481	2·47327	21·9857
1000	500	550·610	1·25918	23·0041	3·61763	42·8539	5·83814
	1000	719·322	1·23651	92·3871	2·47952	133·701	3·74335

Asymptotically as $\rho \to \infty$ it may be seen that V_{eff} goes as $1-(2/\rho)+\alpha^2/\rho^2$, showing that it tends to 1 from below. Tables 1 to 4 give the actual values of the effective maxima (M_1, M_2) and the minimum (m_1) and their locations ρ_{M_1}, ρ_{m_1} and ρ_{M_2} for different values of a, λ, and L, between $\rho=\bar{\rho}\equiv 1+\sqrt{1-a^2}+0{\cdot}0001$, and $\rho=30$.

For a given a and λ as L increases the M_2 increases continuously, whereas M_1 decreases for lower values of a ($\sim 0{\cdot}1$) but increases for other values of a ($\gtrsim 0{\cdot}45$). On the other hand, the effective minimum (m_1) increases as L increases for all a and λ and moves inwards in ρ.

When L is fixed, as λ increases, for all aM_1 increases whereas m_1 and M_2 keep decreasing monotonically. Thus as λ increases the potential well gets flatter and moves outward in ρ. If L and λ are fixed as a increases the entire potential well moves upwards in energy and inwards in ρ. In the equatorial plane we know that the ergosurface corresponds to $\rho=2$. From the figures and tables it is clear that for some set of parameters the entire potential well stays outside the ergosurface (e.g. $a=0{\cdot}1$, $\lambda>300$) while in some other cases it stays completely within the ergosurface (e.g. $a=0{\cdot}9$, $L\geqslant 500$, $\lambda\leqslant 50$). For other set of values part of the potential well stays inside and part outside the ergosurface.

Case 2

The vector potential for the case of a black hole immersed in a uniform magnetic field as given in (11) expressed in dimensionless quantities take the form:

$$A_\tau = -\lambda a\,(1-1/\rho), \quad \lambda = eB_0 m \tag{28}$$

$$\bar{A}_\varphi = \frac{\lambda}{2}\left[\rho^2+a^2\left(1-\frac{2}{\rho}\right)\right]. \tag{29}$$

Substituting these in V_{eff} we get

$$V_{\text{eff}} = \lambda a\,(1-1/\rho) + K/R \tag{30}$$

with K and R as defined earlier.

As we are taking a strictly less than 1, there is no singularity in the vector potential.

Asymptotically we find that

$$V_{\text{eff}} \approx 1 + \lambda a + \left(\frac{\bar{A}_\varphi}{\rho}\right)^2 - \frac{\bar{A}_\varphi L}{\rho} \tag{31}$$

$$\approx 1+\lambda a+O(\rho^2)+\text{constant}.$$

Hence the effective potential increases as the square of the distance for large values of ρ. There are only two extrema (one maximum and one minimum) for the effective potential, which we have tabulated in tables 5 to 8 for different values of a, λ and L. As may be seen from the tables there always exist a potential well, but it is either completely away from the ergosurface ($a=0{\cdot}1$) or only a part of it lies within the ergosurface with the rest outside.

For a given a and λ as L increases the minimum moves outwards in ρ, whereas for fixed a and L as λ increases the minimum moves towards the event horizon. The same thing happens for fixed L and λ as a increases.

5. Orbits

In both the cases we have found existence of well defined potential wells. Naturally only those particles which are confined inside the potential well will have bound orbits. In order to get the actual orbits we integrate the set of equations :

Table 5. $\alpha = 0{\cdot}1$ $\bar{\rho} = 1{\cdot}99508$

λ	L	M	ρ_M	m	ρ_m
	10	—	$< \bar{\rho}$	—	$< \bar{\rho}$
	100	—	$< \bar{\rho}$	—	$< \bar{\rho}$
50	500	69·0159	2·46470	4·62532	4·47162
	1000	166·155	2·61906	5·03626	6·32406
	10	—	$< \bar{\rho}$	—	$< \bar{\rho}$
	100	—	$< \bar{\rho}$	—	$< \bar{\rho}$
150	500	30·1357	2·15137	9·66494	2·58173
	1000	114·066	2·35635	11·5640	3·65093
	10	—	$< \bar{\rho}$	—	$< \bar{\rho}$
	100	—	$< \bar{\rho}$	—	$< \bar{\rho}$
300	500	—	$< \bar{\rho}$	—	$< \bar{\rho}$
	1000	60·2686	2·15136	18·8545	2·58165
	10	—	$< \bar{\rho}$	—	$< \bar{\rho}$
	100	—	$< \bar{\rho}$	—	$< \bar{\rho}$
500	500	—	$< \bar{\rho}$	—	$< \bar{\rho}$
	1000	25·1003	1·99610	25·0477	2·00059
	10	—	$< \bar{\rho}$	—	$< \bar{\rho}$
	100	—	$< \bar{\rho}$	—	$< \bar{\rho}$
1000	500	—	$< \bar{\rho}$	—	$< \bar{\rho}$
	1000	—	$< \bar{\rho}$	—	$< \bar{\rho}$

Table 6. $\alpha = 0{\cdot}45$ $\bar{\rho} = 1{\cdot}893128$

λ	L	M	ρ_M	m	ρ_m
	10	—	$< \bar{\rho}$	—	$< \bar{\rho}$
	100	12·1669	1·91115	11·4500	2·00754
50	500	99·9600	2·20626	18·1985	4·46019
	1000	217·089	2·29252	19·7631	6·31386
	10	—	$< \bar{\rho}$	—	$< \bar{\rho}$
	100	—	$< \bar{\rho}$	—	$< \bar{\rho}$
150	500	74·6676	2·01292	46·7548	2·57409
	1000	184·852	2·14186	49·6245	3·63929
	10	—	$< \bar{\rho}$	—	$< \bar{\rho}$
	100	—	$< \bar{\rho}$	—	$< \bar{\rho}$
300	500	—	$< \bar{\rho}$	—	$< \bar{\rho}$
	1000	149·333	2·01292	83·0231	2·57367
	10	—	$< \bar{\rho}$	—	$< \bar{\rho}$
	100	—	$< \bar{\rho}$	—	$< \bar{\rho}$
500	500	—	$< \bar{\rho}$	—	$< \bar{\rho}$
	1000	121·572	1·91044	112·691	2·00103
	10	—	$< \bar{\rho}$	—	$< \bar{\rho}$
	100	—	$< \bar{\rho}$	—	$< \bar{\rho}$
1000	500	—	$< \bar{\rho}$	—	$< \bar{\rho}$
	1000	—	$< \bar{\rho}$	—	$< \bar{\rho}$

$$\frac{1}{\triangle}\frac{d^2\rho}{d\sigma^2} - \frac{1}{\triangle^2}\left(1 - \frac{\alpha^2}{\rho}\right)\left(\frac{d\rho}{d\sigma}\right)^2 - \left(\frac{1}{\rho} - \frac{\alpha^2}{\rho^4}\right)\left(\frac{d\varphi}{d\sigma}\right)^2 - \frac{2\alpha}{\rho^4}\left(\frac{d\varphi}{d\sigma}\right)\left(\frac{d\tau}{d\sigma}\right) + \frac{1}{\rho^4}\left(\frac{d\tau}{d\sigma}\right)^2 = \frac{1}{\rho^2}\left\{\frac{d\bar{A}_\varphi}{d\rho}\frac{d\varphi}{d\sigma} + \frac{d\bar{A}_\tau}{d\rho}\frac{d\tau}{d\sigma}\right\}, \tag{32}$$

$$\frac{d\varphi}{d\sigma} = \frac{1}{\Delta}\left\{\left(1-\frac{2}{\rho}\right)(L-\bar{A}_\varphi) + \frac{2a}{\rho}(E+A_\tau)\right\} \tag{33}$$

$$\frac{d\tau}{d\sigma} = \frac{1}{\Delta}\left\{\left(\rho^2+a^2+\frac{2a^2}{\rho}\right)(E+A_\tau) - \frac{2a}{\rho}(L-\bar{A}_\varphi)\right\}, \tag{34}$$

Table 7. $a = 0{\cdot}9$ $\bar{\rho} = 1{\cdot}435989$

λ	L	M	ρ_M	m	ρ_m
	10	—	$< \bar{\rho}$	—	$< \bar{\rho}$
	100	32·7177	1·47693	22·8575	2·00754
50	500	172·774	1·53396	35·5685	4·42338
	1000	348·467	1·54506	38·6618	6·28128
	10	—	$< \bar{\rho}$	—	$< \bar{\rho}$
	100	—	$< \bar{\rho}$	—	$< \bar{\rho}$
150	500	167·681	1·50034	82·5349	2·54942
	1000	342·790	1·52416	98·1962	3·60243
	10	—	$< \bar{\rho}$	—	$< \bar{\rho}$
	100	—	$< \bar{\rho}$	—	$< \bar{\rho}$
300	500	161·858	1·46744	123·895	1·84617
	1000	335·362	1·50034	164·553	2·54873
	10	—	$< \bar{\rho}$	—	$< \bar{\rho}$
	100	—	$< \bar{\rho}$	—	$< \bar{\rho}$
500	500	157·224	1·44032	151·016	1·51735
	1000	327·158	1·47686	225·354	2·00083
	10	—	$< \bar{\rho}$	—	$< \bar{\rho}$
	100	—	$< \bar{\rho}$	—	$< \bar{\rho}$
1000	500	—	$< \bar{\rho}$	—	$< \bar{\rho}$
	1000	314·446	1·44032	302·013	1·51672

Table 8. $a = 0{\cdot}99$ $\bar{\rho} = 1{\cdot}141167$

λ	L	M	ρ_M	m	ρ_m
	10	—	$< \bar{\rho}$	—	$< \bar{\rho}$
	100	44·1595	1·16043	25·1348	2·00711
50	500	221·784	1·16599	39·0247	4·41306
	1000	443·833	1·16680	42·4337	6·27213
	10	—	$< \bar{\rho}$	—	$< \bar{\rho}$
	100	43·7661	1·15077	38·2329	1·35232
150	500	221·273	1·16303	90·5889	2·54269
	1000	443·305	1·16521	107·831	3·59218
	10	—	$< \bar{\rho}$	—	$< \bar{\rho}$
	100	43·4183	1·14232	42·7122	1·18158
300	500	220·568	1·15922	136·592	1·84927
	1000	442·546	1·16303	180·653	2·54197
	10	—	$< \bar{\rho}$	—	$< \bar{\rho}$
	100	—	$< \bar{\rho}$	—	$< \bar{\rho}$
500	500	219·729	1·15501	169·483	1·52132
	1000	441·590	1·16041	247·882	2·00077
	10	—	$< \bar{\rho}$	—	$< \bar{\rho}$
	100	—	$< \bar{\rho}$	—	$< \bar{\rho}$
1000	500	218·084	1·14730	202·333	1·25899
	1000	439·458	1·15501	338·776	1·52055

with initial conditions

$$\rho = \rho_0, \quad \varphi = \varphi_0 = 0$$

$$\left(\frac{d\rho}{d\sigma}\right)_0 = \pm \left\{\left(1 + \frac{a^2}{\rho_0^2} + \frac{2a^2}{\rho_0^3}\right)[E+(A_\tau)_0]^2 - \frac{4a}{\rho_0^3}[E + (A_\tau)_0]\,[L - (\bar{A}\varphi)_0] - \left(\frac{1}{\rho_0^2} - \frac{2}{\rho_0^3}\right)[L-(\bar{A}\varphi)_0]^2 - \left(1 - \frac{2}{\rho_0} + \frac{a^2}{\rho_0^2}\right)\right\} \tag{35}$$

$$(A_\tau)_0 = (A_\tau)_{\rho=\rho_0}, \quad (\bar{A}\varphi)_0 = (\bar{A}\varphi)_{\rho=\rho_0}.$$

Figures 8 to 17 give the orbits for the case 1 whereas figures 18 to 26 give the orbits for the case 2. The most important point borne out in either case is that the particle executes Larmor motion (gyration) only outside the ergosurface. This is in fact the reflection of the effect of dragging of inertial frames by the rotating star. For we know that if the particle has to gyrate, then during every Larmor circle the particle angular velocity $(d\varphi/d\sigma)$ will be prograde for one half and retrograde for the other half with respect to the angular velocity of the star. It is well known that in the Kerr geometry the ergosurface is the static limit surface on and behind (towards the event horizon) which no retrograde motion is possible. Thus the particle can gyrate only outside the ergosurface. This fact can also be seen analytically as follows. When a particle gyrates its $(d\varphi/d\sigma)$ has to go through zero for some $\rho=\rho_g$, for which $(d\rho/d\sigma)_{\rho=\rho_g}$ should be real and positive.

$(d\varphi/d\sigma)_{\rho=\rho_g} = 0$ gives

$$(1-2/\rho_g)\,[L-(\bar{A}\varphi)_{\rho=\rho_g}] + \frac{2a}{\rho_g}\,[E+(A_\tau)_{\rho=\rho_g}] = 0. \tag{36}$$

Using this in $(d\rho/d\sigma)^2_{\rho=\rho_g}$ we get

$$(d\rho/d\sigma)^2_{\rho=\rho_g} = \frac{\Delta}{\rho_g^2}\{(1-2/\rho_g)^{-1}\,[E+(A_\tau)_{\rho=\rho_g}]^2 - 1\}.$$

Since $\Delta > 0$, in the region under consideration, $(d\rho/d\sigma)_{\rho=\rho_g}$ will be real if and only if

$$(1-2/\rho_g)^{-1}\,[E+(A_\tau)_{\rho=\rho_g}]^2 > 1 \tag{37}$$

This can be true only for $(1-2/\rho_g) > 0$, or $\rho_g > 2$, i.e. outside the ergosurface.

Another aspect of the dragging appears through the precession of the entire orbit for every revolution. Looking at the actual plots we see that as the magnetic field changes, for a given a and L, the nature of the orbit changes. For example, consider the dipole field (figures 8–12). When $\lambda = 1000$, 500 and 300, both the turning points of the orbit lie outside $\rho = 2$ and thus there is gyration whereas when $\lambda = 150$, and 50, both the turning points are inside $\rho = 2$ and thus there is no gyration. On the other hand, if we consider the cases of figures 13–17, here a, λ and L are kept constant and E alone varies. When E is large, (figures 13 and 14), the potential well is such that the particle moves in and out of the ergosurface without gyrating. As the energy is decreased it will be in the region of the potential well, which is completely

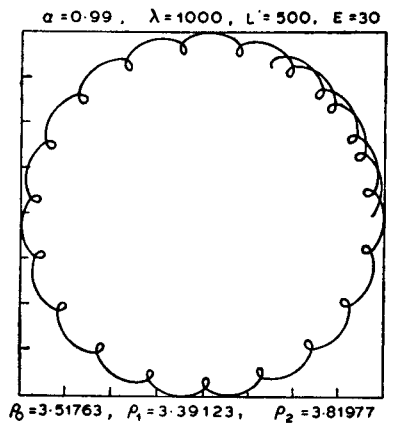

Figure 8.

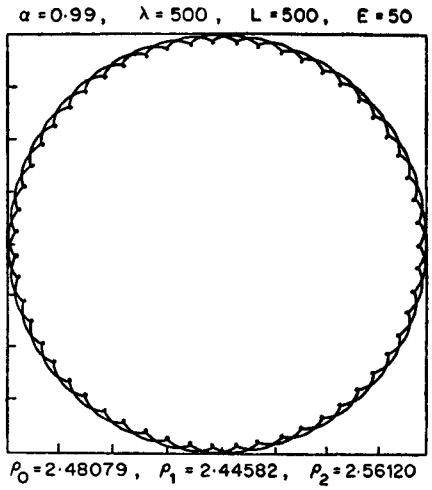

Figure 9.

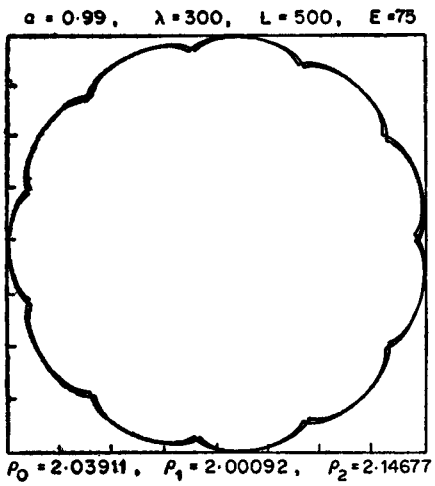

Figure 10.

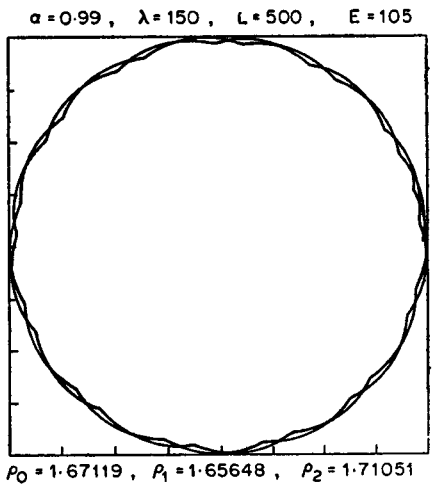

Figure 11.

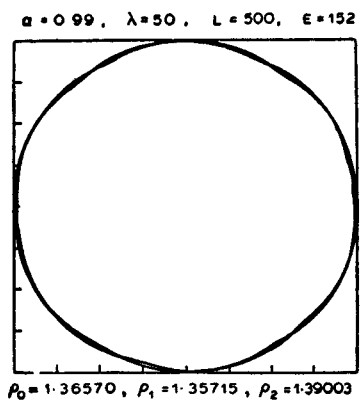

Figure 12.

Figures 8-12. Orbits in the equatorial plane for different values of λ but same α and L (dipole field).

outside $\rho = 2$ and thus the particle gyrates. As we go down in energy towards the potential minimum the Larmor circles get smaller and smaller. Figure 17 depicts the case when the energy is almost near the minimum and thus the orbit looks almost circular. At the potential minimum it is well known that the particle will have a stable circular orbit.

We have similar orbits for the case of the uniform magnetic field too. Here in the cases (figures 18 to 22) for the same a, L and E as λ changes from 50 to 1000 (increasing magnetic field) the motion is such that till $\lambda = 500$ the particle moves in and out of the ergosurface executing gyration while outside, and follows a purely prograde motion inside. For $\lambda = 1000$, the particle is completely within the ergosurface and thus it does not gyrate. Figures 23 to 25 depict the other aspect that for fixed a, λ and L as the energy changes the orbits change. At $E = 320$, the particle is moving in and out of the ergosurface while for $E = 200$ and 100 it stays completely outside the ergosurface executing fully Larmor motion.

6. Concluding remarks

In the foregoing we have considered two types of magnetic fields. The case of the uniform field could correspond to the galactic magnetic field surrounding the compact object. The dipole field considered could correspond to the intrinsic magnetic field of the compact object, if it is not a black hole. In such a case the vector potential is well behaved down to the surface of the star. In the case of a blackhole the dipole will have to be generated by external sources such as current rings exterior to the event horizon. The possible existence of these current rings has been pointed out by Petterson (1975). Our formalism applies to the region outside the current rings which could lie very close to the event horizon.

As had been found earlier in the case of dipole magnetic field on the Schwarzschild background, the essential role that the magnetic field plays is to stabilise the orbits.

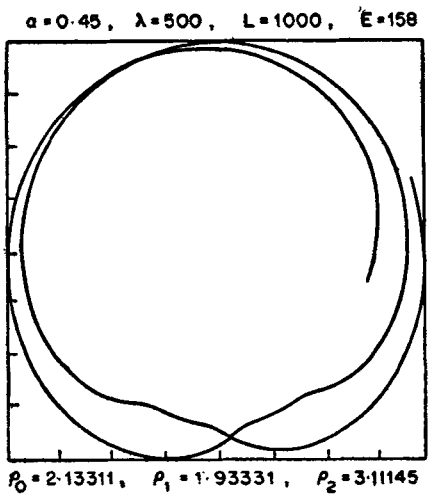

Figure 13.

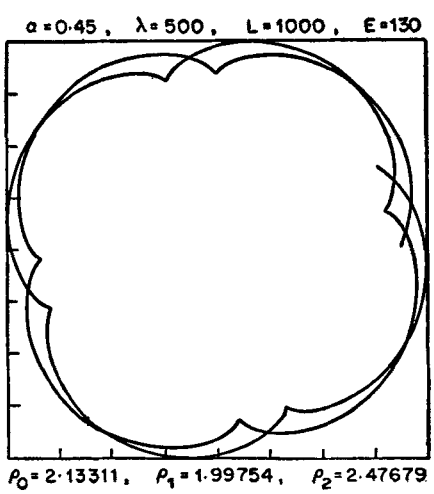

Figure 14.

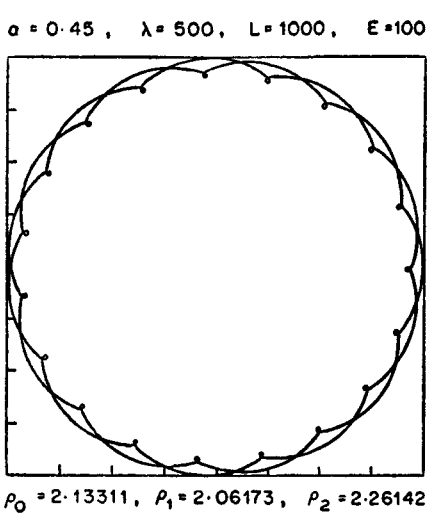

Figure 15.

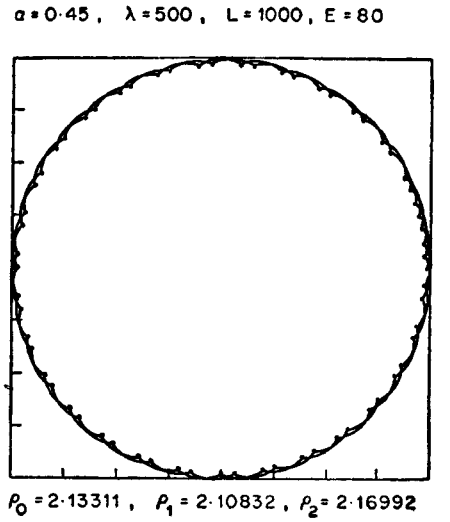

Figure 16.

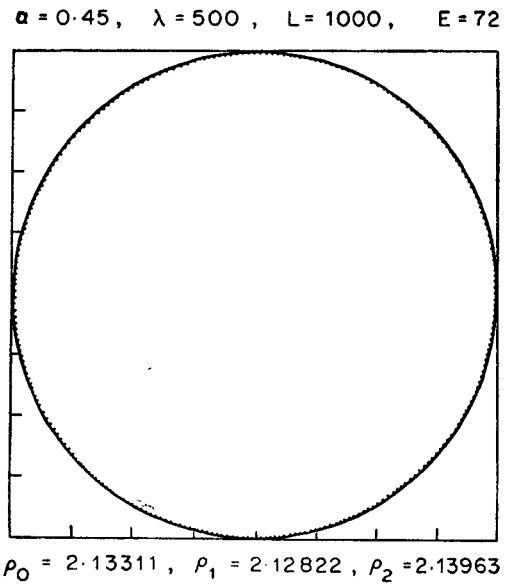

Figure 17.

Figures 13-17. Orbits for different energies but α, λ and L being the same (dipole field) .

Existence of bound orbits depending on the structure of the potential well is similar to the earlier case. However, the important difference is the existence of non gyrating bound orbits within the ergosphere as a result of the dragging of inertial frames due to the rotation of the central star. Charged particles in the two different types of bound orbits—gyrating non-gyrating—could possibly generate significantly different radiation patterns. Further, the above study of orbits could also play an important role while considering plasma discs and particularly the question of transfer of angular momentum. The dynamics of the Penrose energy extraction process

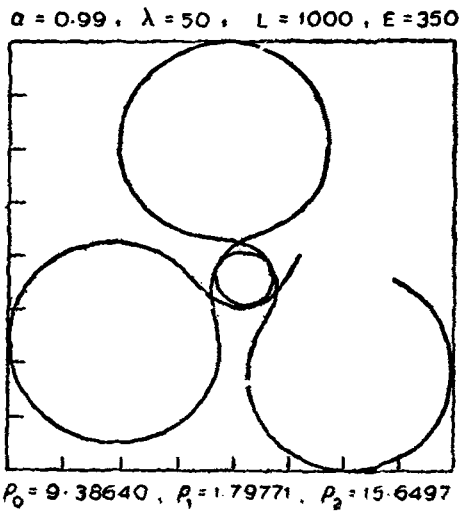

Figure 18.

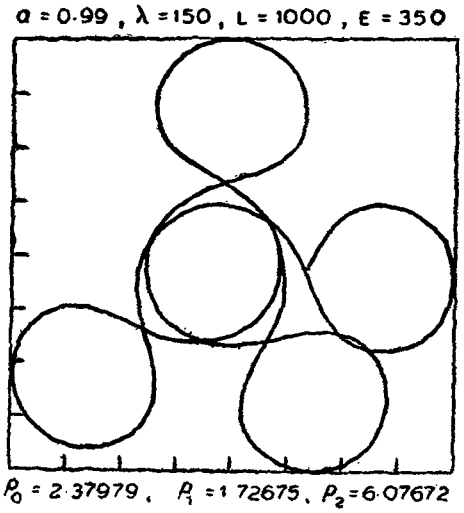

Figure 19.

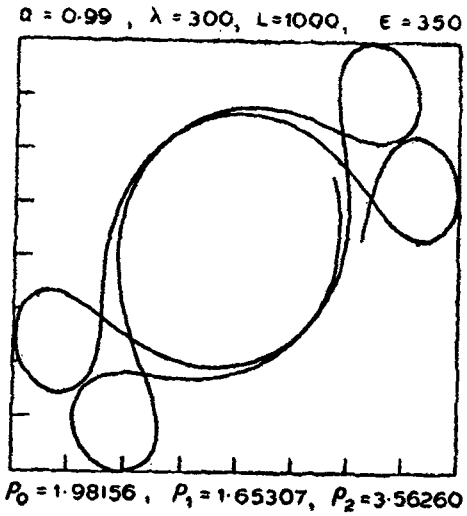

Figure 20.

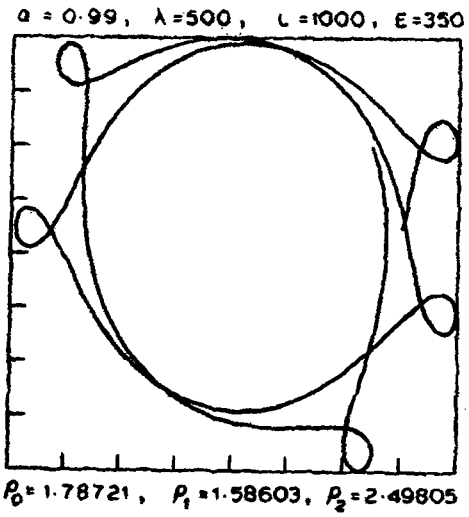

Figure 21.

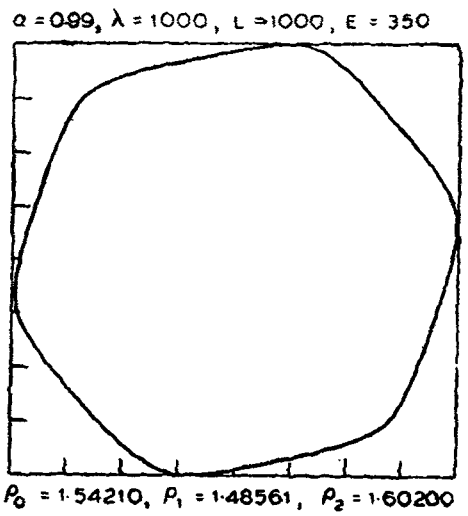

Figure 22.

Figures 18-22. Orbits for different values of λ but same values of L and E (uniform magnetic field).

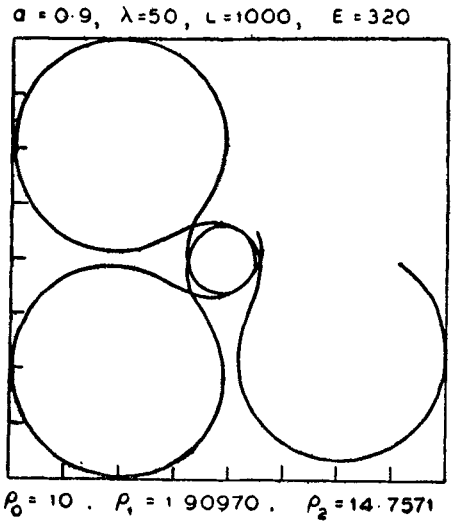

Figure 23.

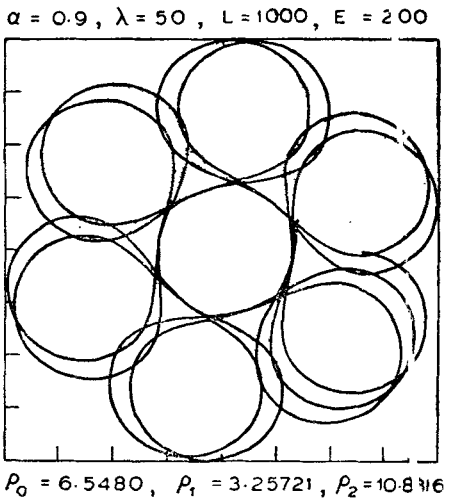

Figure 24.

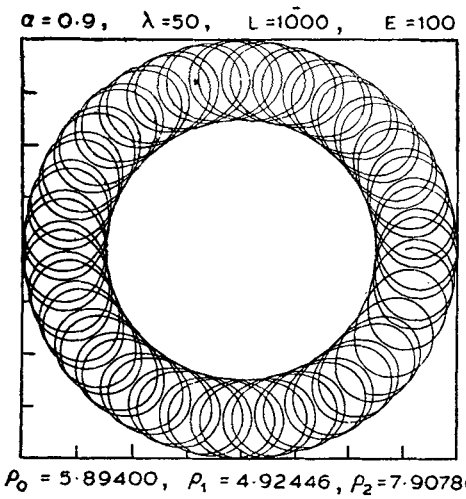

Figure 25.

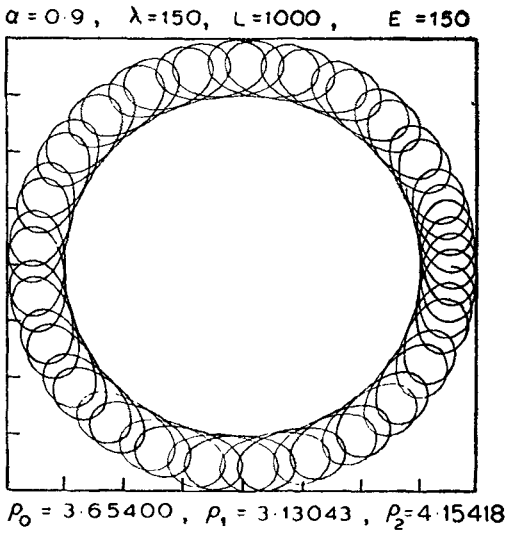

Figure 26.

Figures 23-25. Orbits for different values or energy but same values of α, λ and L (uniform magnetic field).

Figure 26. A typical plot of a gyrating orbit well outside the ergosurface (uniform magnetic field).

through injecting a particle into ergosphere should now be discussed with the help of the details of the possible orbits for different values of energy, angular momentum, magnetic field strength and the Kerr-angular velocity parameter a obtained in the above study.

Acknowledgements

It is a pleasure to thank Dr K S Rao for his valuable help in the numerical computations and Prof R K Varma for useful discussions. This work got started when

one of us (ARP) was visiting the Raman Research Institute and the Centre for Theoretical Studies, Indian Institute of Science, Bangalore, during the summer of 1977. He would like to thank Profs V Radhakrishnan and N Mukunda for the hospitality shown to him at their respective institutions.

References

Barden J M 1972 *Les Houches Lectures Black Holes* eds. Dewitt and Dewitt, p. 219
Bicak J and Stuchlik Z 1976 *Mon. Not. R. Astron. Soc.* **175** 381
Chitre D M and Vishveshwara C V 1975 *Phys. Rev.* **D12** 1538
King A R, Lasota J P and Kundt W 1975 *Phys. Rev.* **D12** 3037
Petterson J A 1975 *Phys. Rev.* **D12** p. 2218
Prasanna A R and Varma R K 1977 *Pramana* **8** 229
Wald R M 1974 *Phys. Rev.* **D10** 1680